Nuclear Physics B303 (1988) 36–56
North-Holland, Amsterdam

TOPOLOGICAL CHARGE AND FERMIONS IN THE TWO-DIMENSIONAL LATTICE U(1) MODEL (I). Staggered fermions

Jan SMIT and Jeroen C. VINK

Institute of Theoretical Physics, Valckenierstraat 65, 1018 XE Amsterdam, The Netherlands

Received 16 October 1987

We investigate various definitions of topological charge within the compact QED_2 model. In particular we study for staggered fermions the charge, $\bar{Q} = \frac{1}{2}\kappa_P m \,\mathrm{Tr}\, \Gamma_5 (\not{D} + m)^{-1}$ and its renormalization factor κ_P.

1. Introduction

Topology and topological charge of quantum gauge fields has been an intriguing subject for some time now, especially after the discovery of a formula that relates the masses of the neutral pseudoscalar mesons to the topological susceptibility of the gluon field [1]. Recently we have derived this formula within the lattice formulation of QCD, with the quark fields represented by either Wilson fermions [2] or staggered fermions [3]. This leads to a definition of topological charge in terms of the fermion fields,

$$\bar{Q} = \kappa_P \hat{Q} = \kappa_P \frac{m}{n_f} \mathrm{Tr}\, \Gamma_5 (\not{D} + m)^{-1}, \tag{1.1}$$

where $(\not{D} + m)^{-1}$ represents the fermion propagator in a given gauge field, Γ_5 represents the Dirac γ_5, m is the mass parameter for the n_f degenerate flavours of quarks and κ_P is a finite renormalization constant. Expressions like (1.1) have appeared in the literature before, without the renormalization factor κ_P, however [4, 5].

In the continuum formulation, (1.1) expresses a relation between the topological charge Q of a gauge field and the zero modes of the Dirac operator $\not{D}$ in this gauge field,

$$Q = \frac{m}{n_f} \mathrm{Tr}\, \gamma_5 (\not{D} + m)^{-1} = n_+ - n_-, \tag{1.2}$$

where n_+ (n_-) is the number of zero modes per flavour with chirality $+1$ (-1). We

0550-3213/88/$03.50

refer to (1.2) as the "Atiyah-Singer index theorem". Obviously, Q is integer here and the apparent mass dependence in (1.2) disappears. On the lattice the theorem does not apply and $\hat{Q}$ is not integer: it needs a finite renormalization and it is m-dependent.

Within QCD we have discussed [2,3] how the required renormalization can be found and argued (for staggered fermions, at least) how the problems related to the m-dependence of $\overline{Q}$ can be circumvented for the ensuing susceptibility. In ref. [6] we have reported numerical results of a pilot study measuring the susceptibility of $\overline{Q}$ in QCD at $\beta = 5.7$, using staggered fermions.

Within QCD it is very hard to investigate the properties of $\hat{Q}$ in great detail: we would like to know the m-dependence of $\hat{Q}$ for $0 \leqslant m \leqslant \infty$, elucidate the renormalization, exhibit the role of the zero modes and see to what extent the index theorem (1.2) is recovered on the lattice. Difficult as this may be in QCD, it can be done in two-dimensional QED (QED_2), which shares essential topological properties with QCD but is computationally far less demanding. In ref. [7] we have started an investigation, using non-trivial smooth gauge fields to search for remnants of the index theorem. As an intermediate step between these trial configurations and the real fluctuating gauge fields of QED_2, we also studied artificially roughened gauge fields there. Here we present a detailed discussion of the properties of $\hat{Q}$ within QED_2, using staggered fermions. Wilson fermions will be considered in a subsequent paper [8]. Some of the preliminary results have been reported in [9].

The remainder is organized as follows. Sect. 2 deals with the compact QED_2 model without fermions, for which we derive some useful exact results on various topological susceptibilities. Sect. 3 deals with $\hat{Q}$: the finite renormalization, the relation with the spectrum of $\not{D}$ and the susceptibility. Sect. 4 contains our conclusions and a discussion of differences between QED_2 and QCD. An appendix contains some details of the computations in sect. 2.

2. Topological susceptibility in the U(1) model

The compact U(1) model is defined on a two-dimensional lattice by the action,

$$S = \beta \sum_n \mathrm{Re}\, U_{12}(x), \qquad \beta = 1/a^2 g^2, \tag{2.1}$$

where a is the lattice distance, g is the bare gauge coupling with the dimension of a mass and $U_{12}(x) \in U(1)$ are the usual plaquette variables. The summation is over lattices sites,

$$x_\mu = n_\mu a, \qquad \text{with } n_\mu = 0, \ldots, N-1 \qquad (\mu = 1,2), \tag{2.2}$$

and periodic boundary conditions are implied. The notation $\Sigma_x \equiv a^2 \Sigma_n$ will also be used.

It is possible to assign topological charge to the gauge field U (see e.g. ref. [10])

$$Q_t = \sum_x q_t(x), \qquad q_t(x) = \frac{1}{2\pi} F_{12}(x), \tag{2.3}$$

where the field strength F_{12} is obtained from the plaquette through

$$U_{12} = e^{-ia^2 F_{12}}, \tag{2.4}$$

with the restriction $a^2 F_{12} \in (-\pi, \pi]$.

An alternative "naive" definition which reduces to Q_t for $a \to 0$ is

$$Q_n = \sum_x q_n(x), \qquad q_n(x) = \frac{-1}{2\pi a^2} \operatorname{Im} U_{12}(x). \tag{2.5}$$

Contrary to q_t, q_n is a continuous function of the gauge field; however, in general Q_n is not an integer.

We are interested in the susceptibility χ of these charges,

$$\chi_{t,n} = \sum_x \langle q_{t,n}(x) q_{t,n}(0) \rangle = \langle Q_{t,n}^2 \rangle L^{-2}. \tag{2.6}$$

The brackets denote the path integral average with the action (2.1) and $L^2 = a^2 N^2$ is the space-time volume. On dimensional grounds, we can write

$$\chi_{t,n} = \tilde{c}_{t,n}(\beta, N) g^2 / 4\pi^2, \tag{2.7a}$$

where the normalization is such that for $\beta \to \infty$

$$\lim_{N \to \infty} \tilde{c}_{t,n}(\beta, N) = c_{t,n}(\beta) = 1 + O(\beta^{-1}) \tag{2.7b}$$

as can be verified from the results to be presented shortly. Similarly, the string tension σ for $N \to \infty$ can be expressed as

$$\sigma = \tfrac{1}{2} c_\sigma(\beta) g^2, \tag{2.8}$$

with $c_\sigma(\beta) = 1 + O(\beta^{-1})$ for $\beta \to \infty$.

For finite values of β there may be a scaling behaviour in which case the c's have the same β-dependence: $c_{t,n}/c_\sigma \approx 1$, where the deviation from 1 is much less than for the individual c's. This possibility can be investigated explicitly, since the functions $\tilde{c}_{t,n}(\beta, N)$ can be evaluated exactly. Details of this computation are in the

appendix, where it is shown that for $N \to \infty$

$$4\pi^2 a^2 \chi_t = \frac{\pi^2}{3} + 4 \sum_{k=1}^{\infty} \frac{(-1)^k}{k^2} \tilde{I}_k(\beta), \tag{2.9a}$$

$$4\pi^2 a^2 \chi_n = \beta^{-1} \tilde{I}_1(\beta), \tag{2.9b}$$

$$\tilde{I}_k(\beta) = I_k(\beta)/I_0(\beta), \tag{2.9c}$$

with $I_k(\beta)$ the modified Bessel function of order k. From (2.9b) and (2.7) one may recognize that $c_n(\beta)$ is equal to the average plaquette

$$\langle \cos a^2 F_{12} \rangle = \tilde{I}_1(\beta) = c_n(\beta), \tag{2.10}$$

which shows that χ_n approaches its continuum limit value from below. The string tension can be inferred from the average plaquette, since Wilson loops obey an exact area law for $N \to \infty$:

$$a^2\sigma = -\log\big(\tilde{I}_1(\beta)\big), \qquad c_\sigma = -2\beta \log \tilde{I}_1. \tag{2.11}$$

For $\beta \to \infty$ one verifies that $\sigma \sim \frac{1}{2}g^2$, for finite β we define a renormalized coupling

$$g_R^2 = c_\sigma(\beta) g^2, \tag{2.12}$$

such that $\sigma = \frac{1}{2} g_R^2$ and use g_R as a scale for $\chi_{t,n}$.

Fig. 1 shows plots of $4\pi^2 \chi_{t,n}/g_R^2$. It is seen that $4\pi^2 \chi_t / g_R^2 \approx 1$ for $\beta \gtrsim 2$ and we interpret this as scaling. The precocious scaling for $\beta = 1.2$–2.4 was also found in ref. [10]. The naive susceptibility does not follow this scaling behaviour, only for $\beta \to \infty$, $4\pi^2 \chi_n / g_R^2 \sim 1$. In fig. 1 we have also plotted $\langle Q_n(UV) \rangle / Q_v$. Here the charge Q_n is averaged over the fluctuating gauge field U, multiplied by an external field V. The smooth field V is obtained in a well-defined way [7] from a continuum gauge field v, which is smooth on the scale of the lattice distance and has topological charge Q_v. For these gauge fields V one finds

$$Q_v = Q_t(V) = Q_n(V) + O(1/N^2). \tag{2.13}$$

It is seen that $\langle Q_n(UV) \rangle \to Q_v$ for $\beta \to \infty$, but for finite β there is a β-dependent reduction. This can be considered as a scaling violation, since $\langle Q_n(UV) \rangle$ has dimension zero and should scale as a constant.

To improve the scaling behaviour of χ_n, we propose a multiplicative renormalization of q_n, such that $\langle \overline{Q}_n(UV) \rangle = Q_v$ for the renormalized charge

$$\overline{Q}_n = \kappa_n(\beta) Q_n. \tag{2.14}$$

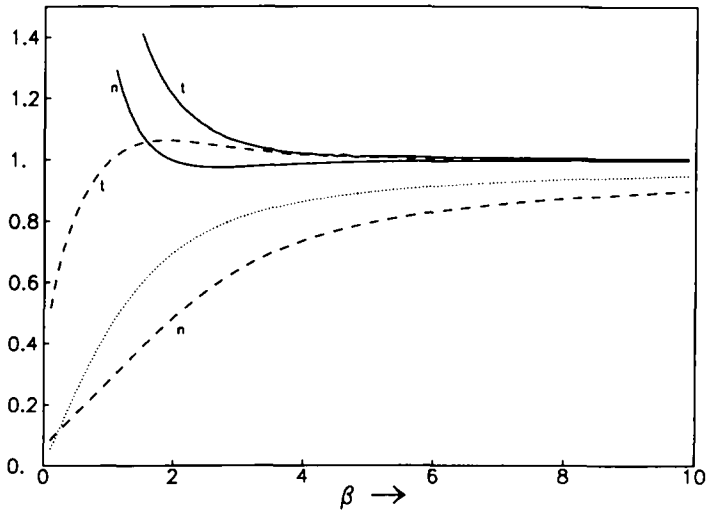

Fig. 1. Scaling behaviour. The full (dashed) curve represents the renormalized (unrenormalized) naive susceptibility, indicated by n and the topological susceptibility, indicated by t, in units of $g_R^2/4\pi^2$. The dotted curve represents $\langle Q_n(UV)\rangle Q_v^{-1}$.

This implies

$$\kappa_n(\beta) = Q_v/\langle Q_n(UV)\rangle . \tag{2.15}$$

We can evaluate

$$\langle Q_n(UV)\rangle = \frac{-1}{2\pi a^2}\sum_n \langle \mathrm{Im}(U_{12}(x)V_{12}(x))\rangle = Q_n(V)\langle \mathrm{Re}\, U_{12}\rangle , \tag{2.16}$$

where it was used that $\langle \mathrm{Im}\, U_{12}\rangle = 0$. Using (2.13) and (2.15) it follows that for $N \to \infty$

$$\kappa_n = \langle \mathrm{Re}\, U_{12}\rangle^{-1}, \tag{2.17}$$

i.e., the renormalization factor κ_n is the inverse of the average plaquette. Note that for $N \to \infty$ the apparent V dependence of κ_n in (2.15) disappears. The susceptibility of the renormalized charge, $\bar{\chi}_n = \kappa_n^2 \chi_n$, has a remarkably improved scaling behaviour. It can be seen in fig. 1 that $4\pi^2\bar{\chi}_n/g_R^2 \approx 1$ for $\beta \gtrsim 2$, whereas the unrenormalized χ_n deviates significantly from one in this regime.

We can also compare the renormalized naive charge $\bar{Q}_n$ with Q_t for individual configurations. As a measure for the average difference $(\bar{Q}_n - Q_t)/Q_t$ we have computed

$$d = \left[\frac{\langle (\bar{Q}_n - Q_t)^2\rangle}{\langle Q_t^2\rangle}\right]^{1/2} \tag{2.18}$$

which can be evaluated exactly using the method outlined in the appendix. For $\beta \gtrsim 2$ we find

$$d \approx 0.5\beta^{-1}. \tag{2.19}$$

The absolute deviation between $\overline{Q}_n$ and Q_t however, also depends on N. Using $\langle Q_t^2 \rangle \approx (4\pi^2\beta)^{-1}N^2$ it follows that $\langle (\overline{Q}_n - Q_t)^2 \rangle^{1/2} \approx 0.08\beta^{-3/2}N$. Taking $N \to \infty$ at fixed β implies that $\overline{Q}_n$ fluctuates increasingly far from the integers Q_t. Harmless as this is for the susceptibility, one may prefer to avoid it by taking the limits $N \to \infty$, $\beta \to \infty$ such that $\langle Q_t^2 \rangle = O(1)$ remains fixed. This means keeping the physical volume L^2 fixed.

One may wonder how the renormalization procedure (2.14), (2.15) would work out for the topological charge Q_t. Since the unrenormalized charge already leads to a susceptibility which scales for $\beta \gtrsim 2$, one would expect that the renormalization factor $\kappa_t \approx 1$. This can be verified by direct computation of $\kappa_t = \langle Q_t(UV) \rangle^{-1} Q_v$ for $N \to \infty$. As seen in fig. 1, the renormalized susceptibility $\bar{\chi}_t = \kappa_t^2 \chi_t$ hardly differs from χ_t for β in the scaling region.

Apart from scaling violations due to the finite lattice distance, there are also corrections due to the finite volume that one is forced to use in numerical computations. In order to get an idea of the size of these effects, we have computed $\chi_{t,n}$ for finite N, using the expressions derived in the appendix. Fig. 2 shows the N dependence of $4\pi^2 \chi_{t,n} g_R^{-2}$ (g_R is evaluated for $N \to \infty$). It is seen that there is an abrupt crossover to the region where finite-N effects are dominant. For $N^2 \gtrsim 18\beta$ finite-N effects are negligible. In terms of the correlation length $\xi = (a^2\sigma)^{-1/2}$ ($\approx (2\beta)^{1/2}$ for $\beta \gtrsim 2$) this bound is $N \gtrsim 3\xi$.

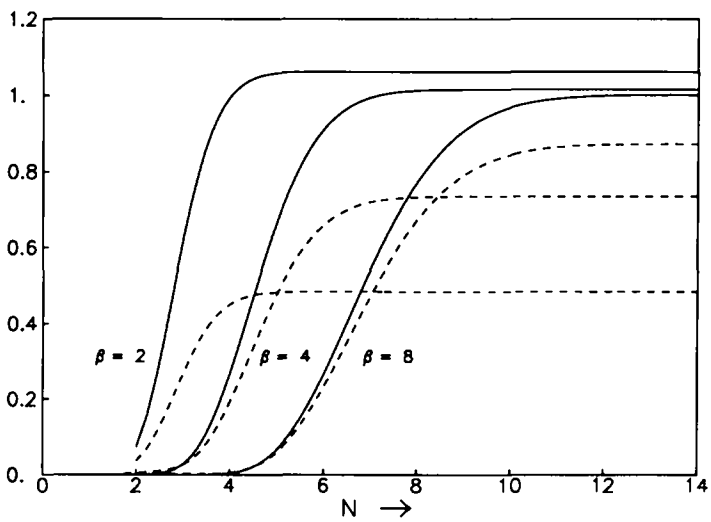

Fig. 2. Finite volume effects. The full (dashed) curve represents the topological (naive) susceptibility.

3. Staggered fermions and topological charge

In this section we use staggered fermions to evaluate the topological charge. The staggered Dirac operator with a mass term can be written as

$$(\not{D}+m)(x,y)=\frac{1}{2a}\sum_{\mu}\eta_{\mu}(x)\big[U_{\mu}(x)\delta(x+a_{\mu}-y)-U_{\mu}^{*}(y)\delta(y+a_{\mu}-x)\big]$$

$$+m\delta(x-y), \tag{3.1}$$

with $\eta_1(x)=1$, $\eta_2(x)=(-1)^{x_1/a}$ and m the quark mass parameter. The Dirac γ_5 matrix is represented by a hermitian two-link operator

$$\Gamma_5(x,y)=-\tfrac{1}{2}i(\Gamma_1\Gamma_2-\Gamma_2\Gamma_1)(x,y),$$

$$\Gamma_{\mu}(x,y)=\tfrac{1}{2}\eta_{\mu}(x)\big[U_{\mu}(x)\delta(x+a_{\mu}-y)+U_{\mu}^{*}(y)\delta(y+a_{\mu}-x)\big]. \tag{3.2}$$

With these notations the unrenormalized "fermionic" topological charge is written as

$$\hat{Q}=\tfrac{1}{2}m\,\mathrm{Tr}\,\Gamma_5(\not{D}+m)^{-1}. \tag{3.3}$$

There is a factor $\frac{1}{2}$, because the staggered Dirac operator (3.1) for $a\to 0$ describes 2 flavours of quarks.

The eigenfunctions and eigenvalues of the Dirac operator can be used to elucidate the connection between fermions and the topological charge. In the continuum formulation there is the Atiyah-Singer index theorem (1.2), relating the charge to the zero modes of the Dirac operator. On the lattice there are remnants of this picture [7]. The eigenvalue equation for the anti-hermitian $\not{D}$ can be written as

$$\not{D}f_s=i\lambda_s f_s, \qquad a\lambda_s\in[-2,2],$$

$$f_s^{\dagger}f_t=\delta_{st}. \tag{3.4}$$

Using these eigenfunctions, $\hat{Q}$ can be represented as [7]

$$\hat{Q}=\tfrac{1}{2}\sum_{s}r_s\frac{m^2}{\lambda_s^2+m^2}, \tag{3.5}$$

where

$$r_s=f_s^{\dagger}\Gamma_5 f_s. \tag{3.6}$$

We have chosen to evaluate $\hat{Q}$ numerically using this spectral representation, i.e. for a given gauge field U we compute all eigenvalues and eigenfunctions of $\not{D}(U)$

and use (3.6) and (3.5) to obtain $\hat{Q}(U)$. This approach has the advantage that $\hat{Q}$ can be evaluated for as many values of m as desired and furthermore the contribution of the various eigenmodes can be studied explicitly. We have restricted ourselves to $N \leqq 16$.

In order to evaluate expectation values involving $\hat{Q}(U)$, we resort to the Monte Carlo method. We have generated gauge field ensembles at $\beta = 1, 2, 3, 4$ and 8. For $\beta \leqslant 4$ we use a conventional 8-hit Metropolis algorithm but for $\beta = 8$ this local updating process is not capable of taking the gauge field from one topological sector to another. To cure this, a non-local updating $U \to U'$ is supplied each four sweeps that changes the topological charge by ± 1. This is achieved by multiplying the old field U with the field V, carrying charge $Q_t = Q_v = +1$ or -1, chosen with equal probability. The new field $U' = UV$ is accepted or rejected in the usual way by the Metropolis procedure.

Some statistics: at $\beta \leqq 4$ we generated 512 configurations on a $N = 8$ lattice, separated by 10β sweeps and discarding 2500β sweeps to equilibrate the field. At $\beta = 8$ we use a larger lattice $N = 12$ and 100 configurations. In order to see possible finite size effects we generated 32 configurations at $\beta = 3$ and $N = 16$. Statistical errors are estimated using a binning procedure.

3.1. THE CHARGE OF SMOOTH FIELDS: $\hat{Q}(V)$

First the charge of smooth fields V is considered. To indicate explicitly all variables, we use the notation*

$$\hat{Q}(V) = Q_v F(am, N, \beta, v), \qquad \beta = \infty, \tag{3.7}$$

where $\beta = \infty$ indicates that $\hat{Q}(V)$ may be considered as the limit of $\langle \hat{Q}(UV) \rangle$ for $\beta \to \infty$ at fixed N and v is the continuum gauge field with charge Q_v that leads to the lattice field V. In the limit $N \to \infty$ with $L = aN$ fixed, the function F is independent of v. To see this the mass dependence of F is written as a power series in $(am)^{-2}$, which converges for $am > 2$,

$$F(am, N, \infty, v) = \frac{1}{2Q_v} \sum_{k=1}^{\infty} \operatorname{Tr} \Gamma_5 \left(\frac{\not{p}}{am} \right)^{2k}. \tag{3.8}$$

The $k = 0$ term is absent since $\operatorname{Tr} \Gamma_5 = 0$. For $k = 1, 2, \ldots$

$$\tfrac{1}{2} \operatorname{Tr} \Gamma_5 \not{p}^{2k} = c_k Q_n^{(k)}, \tag{3.9}$$

with $Q_n^{(k)}$ a "naive" expression for the topological charge and c_k a numerical constant. For $k = 1$, $Q_n^{(1)} \equiv Q_n$ of sect. 2 and $c_1 = \frac{1}{4}\pi$. In the limit $N \to \infty$,

* Note that the notation here differs slightly from ref. [3].

$Q_n^{(k)} \to Q_v$ for arbitrary fixed k and the result follows,

$$\lim_{N\to\infty} F(am, N, \infty, v) = \sum_{k=1}^{\infty} c_k (am)^{-2k}. \tag{3.10}$$

For $am \leqq 2$, F is obtained from (3.10) by analytical continuation. On finite lattices this independence of v is valid for gauge fields that are sufficiently smooth on the lattice scale.

In numerical work we specialize to smooth gauge fields with a constant field strength, the same as those used in ref. [7]. The above result shows that this introduces no bias, provided that N is sufficiently large. For these constant field strength configurations we have found in ref. [7] that $\not{D}$ has $2|Q_v|$ "zero modes" for which $\lambda_s \approx 0$ and $r_s \approx \operatorname{sgn} Q_v$; the nonzero modes have $r_s \approx 0$. Consequently, $\hat{Q}(V) \approx Q_v$ for small am. In the limit $N \to \infty$ (L fixed) the above approximate equalities become exact and then they are in accordance with the Atiyah-Singer index theorem. The am dependence of F for $Q_v = 1$ and $N = 8, 16$ is shown in fig. 3 (two upper curves). Comparison of the curves for $N = 8$ and $N = 16$ gives an idea of finite N effects. The Q_v dependence for these constant field strength gauge fields may give an idea of the v dependence at these N values. From ref. [7], eqs. (3.10)–(3.11) it can be inferred that for small am and $N \geqq 8$,

$$F(am, N, \infty, v) \simeq 1 - 3.2 Q_v/N^2 - 1.2 a^2 m^2 + \cdots, \tag{3.11}$$

which shows that for $N \to \infty$ the Q_v dependence disappears.

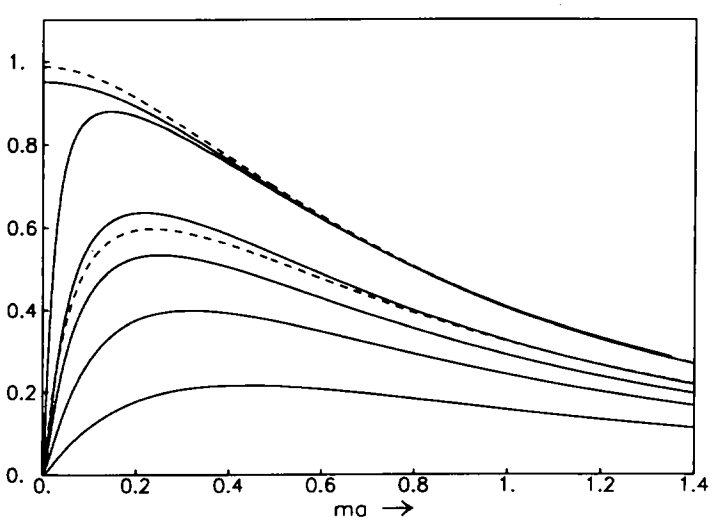

Fig. 3. Mass dependence of $\langle \hat{Q}(UV) \rangle Q_v^{-1}$. The full curves are for $N = 8$, $\beta = 1$ (lowest curve), 2, 3, 4, 8 and ∞ (top curve). The dashed curves are for $N = 16$, $\beta = 3$ and $\beta = \infty$. The statistical errors are: 4% ($\beta = 1$–4, $N = 8$), 9% ($\beta = 8$, $N = 12$) and 15% ($\beta = 3$, $N = 16$).

3.2. THE AVERAGE CHARGE $\langle \hat{Q}(UV) \rangle$

In sect. 2 it was demonstrated how the average external charge $\langle Q_n(UV) \rangle$ can be used to obtain a renormalized charge $\overline{Q}_n$, such that the susceptibility $\overline{\chi}_n$ has an improved scaling behaviour. We will use a similar procedure for $\hat{Q}$. The average external charge can be written as

$$\langle \hat{Q}(UV) \rangle = Q_v F(am, N, \beta, v). \tag{3.12}$$

For $\beta \to \infty$ the function F was introduced in (3.7) and in this limit it is independent of v (for sufficiently large N). We will now argue that this independence of v extends to finite values of β, in the scaling region. To make this plausible we expand F in $(am)^{-2}$ as in (3.8):

$$F(am, N, \beta, v) = \frac{1}{Q_v} \sum_{k=1}^{\infty} c_k \langle Q_n^{(k)}(UV) \rangle (am)^{-2k}. \tag{3.13}$$

We assume that

$$\kappa_n^{(k)} := Q_v / \langle Q_n^{(k)}(UV) \rangle, \qquad N \to \infty \tag{3.14}$$

is independent of v. For $k = 1$ this assumption is valid, as was demonstrated in sect. 2, eqs. (2.15)–(2.17). Combining (3.14) and (3.13) it follows that

$$F(am, \infty, \beta, v) = \sum_{k=1}^{\infty} c_k \kappa_n^{(k)} (\beta)^{-1} (am)^{-2k}, \tag{3.15}$$

which is independent of v. In fig. 3 we show the am dependence of F for $\beta = 1$–4 and 8, using an external field V with constant field strength and $Q_v = 1$. It is seen how for increasing β the curves approach the $\beta = \infty$ curve.

To exhibit finite N effects, we have also used a larger lattice, $N = 16$, to evaluate F for $\beta = 3$. Here the average $\langle \hat{Q}(UV) \rangle$ is estimated from an ensemble of 30 configurations chosen such that Q_t averaged over this ensemble is zero. On a small ensemble, the statistical fluctuations from the $Q \neq 0$ sectors are large and we imposed this constraint in order to avoid a bias in the average $\langle \hat{Q}(UV) \rangle$. The curve for $N = 16$ is reasonably close to the curve for $N = 8$.

A striking difference between the finite-β curves and the $\beta = \infty$ curves is the behaviour for $am \to 0$; for $\beta = \infty$, $F \to 1$ whereas for finite β, $F \to 0$. The different behaviour for $\beta < \infty$ can be clarified using the spectral representation (3.5). For small am the "zero modes" dominate:

$$\hat{Q} = \tfrac{1}{2} {\sum_s}' r_s \frac{m^2}{\lambda_s^2 + m^2} + \cdots, \tag{3.16}$$

where the sum is over the "zero modes" and the dots indicate the non-zero mode contributions.

For the smooth fields V ($\beta = \infty$) there are exact zero modes. However, for the fluctuating gauge fields ($\beta < \infty$) the eigenvalues of the "zero modes" shift to non-zero values (whence the name "zero mode shift"). For example, at $\beta = 4$ the variance of the "zero mode" eigenvalues $\langle (a\lambda_0)^2 \rangle = 0.004$. As a result of the zero mode shift, $\hat{Q} \to 0$ and $F \to 0$ for $am \to 0$.

Apart from the zero mode shift effect, there is an overall reduction of F for finite β. This is also related to the behaviour of the zero modes: it turns out that the zero mode residues $|r_0|$ are reduced for finite β. We find $\langle |r_0| \rangle \approx 1 - 1.1\beta^{-1}$ ($\beta \gtrsim 2$). We should remark that for finite β, it is no longer obvious which modes are "zero modes". The quoted values for $\langle (a\lambda_0)^2 \rangle$ and $\langle |r_0| \rangle$ were obtained using the criterion

$$|a\lambda_0| < 0.2 \qquad \text{and} \qquad |r_0| > 0.3 \tag{3.17}$$

to select the "zero modes". We will discuss the behaviour of $(a\lambda_0, r_0)$ for the zero modes in more detail later.

For $\beta \to \infty$ we expect that $F \to 1$ for all physical values of m (i.e. values am of order $\beta^{-1/2}$). This is not obvious, since the finite β curves approach the $\beta = \infty$ curve non-uniformly in am. To investigate the limit $\beta \to \infty$ more precisely, we define a scaling window (y_-, y_+) for F, such that F varies less than a fraction $\frac{1}{2}\delta$ for am values inside this window: $F_{\max} - \frac{1}{2}\delta < F(am, N, \beta, v) < F_{\max}$ for $y_- < am < y_+$. It is natural to choose the scaling window around the maximum of F, which is reached at $am = y_0$, say. We find numerically that $y_0 \simeq 0.4\beta^{-1/2}$. For increasing β the scaling window may eventually cover all physical values of m: $y_-\beta^{1/2} \to 0$ and $y_+\beta^{1/2} \to \infty$ for $\beta \to \infty$. Since there is a uniform β dependence of F for $am > y_0$ one can verify this behaviour of y_+ using the am dependence of F in the limit $\beta = \infty$, given in (3.11). For small am, we have to check numerically, whether y_- approaches 0 sufficiently fast as $\beta \to \infty$. We find $y_-\beta^{1/2} = 0.23$, 0.22 and 0.17 ($\beta = 3$, 4, and 8) at $\frac{1}{2}\delta = 0.1$. We used a rather large δ to make y_+, y_- less sensitive to the statistical error on F. The data indicate that $y_-\beta^{1/2}$ approaches zero slowly for $\beta \to \infty$. The vanishing of the zero mode shift effect is also illustrated by the β dependence of the variance of the zero mode eigenvalues; for $\beta = 3$, 4 and 8 we find $\langle (a\lambda_0)^2 \rangle \beta = 0.024$, 0.017 and 0.012. Note that even for $\beta = 8$, the lower boundary of the scaling window in physical units is comparatively large: $m/g > y_-\beta^{1/2} = 0.17$. Spectrum computations, however, are typically performed at smaller mass values in the range $0.01 \lesssim m/g \lesssim 0.2$ [12]. We should caution that the numbers for y_- and $\langle \lambda_0^2 \rangle$ are obtained on small lattices ($N = 8$). Even though our (limited) experience with larger lattices ($N = 16$) gives no reason to suspect large finite N effects, it may be that on still larger lattices there is a qualitatively different picture, e.g. y_- may vanish like β^{-1}.

Unfortunately, the rate at which the scaling window enfolds to $(0, \infty)$ is very slow and $y\_\beta^{1/2} \approx 0$ requires large $\beta \gg 8$. In this β-regime $F_{\max} \approx 1$. This leaves us with two alternatives: either use large β, such that $\hat{Q}$ is m-independent in a wide scaling window and $F_{\max} \approx 1$ or we use smaller β, where we are faced with $F_{\max} < 1$ and a strong m-dependence of $\hat{Q}$. We will discuss next how these problems for small β can be overcome to some extent by using a suitable m-dependent renormalization of $\hat{Q}$.

3.3. RENORMALIZED CHARGES

The charges $\hat{Q}$ for individual configurations show a similar m-dependence as the average $\langle \hat{Q}(UV) \rangle$. This suggests that the function $F(am, N, \beta, v)$ can be used to reduce the m-dependence of $\hat{Q}$. In fact, we may argue that the renormalized charge,

$$Q_{\text{int}} = F^{-1}\hat{Q}, \tag{3.18}$$

is approximately mass independent for not too small values of am. The argument uses the expansion of $\hat{Q}$ in terms of the "naive" charges $Q_{\text{n}}^{(k)}$ [cf. (3.13)] and it generalizes the renormalization procedure for $Q_{\text{n}}^{(1)}$ described in sect. 2 to all k. We will assume that the renormalized charges

$$\overline{Q}_{\text{n}}^{(k)} = \kappa_{\text{n}}^{(k)} Q_{\text{n}}^{(k)} \tag{3.19}$$

exert small fluctuations round the integer Q_{t},

$$\overline{Q}_{\text{n}}^{(k)} \approx Q_{\text{t}}, \tag{3.20}$$

for typical configurations U. ($\kappa_n^{(k)}$ is defined in (3.14).) With $\overline{Q}_{\text{n}} \approx Q_{\text{t}}$ we mean $|\overline{Q}_{\text{n}} - Q_{\text{t}}|/Q_{\text{t}} \ll 1$. For $k = 1$ the behaviour (3.20) was verified in (2.19) and it leads to the equality $\bar{\chi}_{\text{n}} \simeq \chi_{\text{t}}$ for $\beta \gtrsim 2$. Under the above assumption it follows that

$$\hat{Q} = \sum_k c_k Q_{\text{n}}^{(k)} (am)^{-2k} = \sum_k c_k \kappa_{\text{n}}^{(k)-1} \overline{Q}_{\text{n}}^{(k)} (am)^{-2k}$$

$$\approx Q_{\text{t}} \sum_k c_k \kappa_{\text{n}}^{(k)-1} (am)^{-2k} = F Q_{\text{t}}. \tag{3.21}$$

In the last equality we used (3.15).

Hence $Q_{\text{int}} \approx Q_{\text{t}}$ in the large am region. For the non-local (large k) charges $\overline{Q}_{\text{n}}^{(k)}$ the fluctuations around Q_{t} presumably are much larger than for $k = 1$. This results in a residual m-dependence of Q_{int} for small m, in particular the zero mode shift effect depends on the particular configuration U and cannot be cancelled by the average effect incorporated in F.

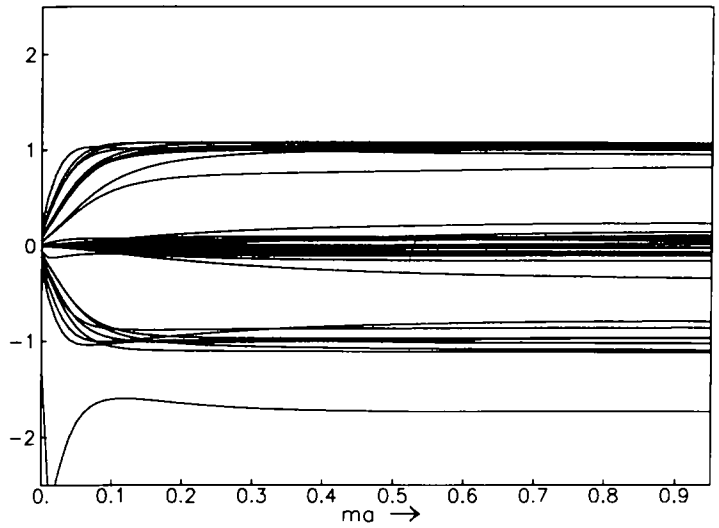

Fig. 4. Mass dependence of $Q_{\rm int}$. The curves show the mass dependence of $Q_{\rm int}$ for 36 configurations at $\beta = 4$, $N = 8$.

These expectations are born out by our numerical results. For the bulk of the configurations at $\beta \geqslant 4$ we find that for $am \gtrsim y_-$, $Q_{\rm int}$ is remarkably constant and close to the integer $Q_{\rm t}$. At $\beta \leqslant 3$ there is a stronger m-dependence and the $Q_{\rm int}$'s digress further away from integers. In the zero mode shift region, $am \lesssim y_-$, the $Q_{\rm int}$'s show a larger m-dependence and stronger fluctuations. This behaviour is demonstrated in fig. 4 where we show $Q_{\rm int}$ of 36 configurations at $\beta = 4$. The value of y_- (for $\frac{1}{2}\delta = 0.1$ and $\beta = 4$) was quoted before: $y_- = 0.11$; it is seen that for most gauge fields, $Q_{\rm int}$ is roughly constant for even smaller values of am. Apparently the zero mode shift effect is to some extent cancelled by the renormalization (3.18).

It is clear from fig. 4 that essentially only charges $|Q_{\rm int}| \lesssim 2$ occur at $\beta = 4$ and $N = 8$. The typical deviation from integers is small. If we would increase the lattice size, the same phenomenon as discussed for $\overline{Q}_{\rm n}$ would occur: the absolute deviations, $Q_{\rm int} - Q_{\rm t}$, would grow $\propto N$ whereas the relative deviations remain small.

The mass independence of $Q_{\rm int}$ leads to a relation between the zero modes of $\not{D}$ and the topological charge $Q_{\rm t}$ of the gauge field. By choosing am just outside the zero mode shift region, $Q_{\rm int}$ can be expressed in terms of the zero modes,

$$\overline{Q} := Q_{\rm int}(y_-) \approx F(y_-, N, \beta, v)^{-1} \tfrac{1}{2} {\sum_s}' r_s ,$$

$$F(y_-, N, \beta, v) \approx \langle |r_0| \rangle , \tag{3.22}$$

where the non-zero mode contribution has been neglected. This leads to

$$\overline{Q} \approx \langle |r_0| \rangle^{-1} \tfrac{1}{2} \sum_s{}' r_s . \tag{3.23}$$

By choosing $am \to \infty$ we can relate $\overline{Q}$ to Q_t:

$$\overline{Q} \approx Q_{\text{int}}(am = \infty) = \overline{Q}_n \approx Q_t . \tag{3.24}$$

For $\beta \to \infty$, $\langle |r_0| \rangle \to 1$ and we recover the continuum result (for two flavours) expressed by the index theorem, with the proviso that N and β are such that $\langle Q^2 \rangle = \mathrm{O}(1)$.

3.4. SPECTRUM OF $\not{\phi}$

Since the spectrum $\{\lambda_s, r_s\}$ of $\not{\phi}$ is explicitly computed, we can investigate to what extent the continuum features are present. In the continuum with two flavours there are non-zero modes with ($\lambda_s \neq 0$, $r_s = 0$) and zero modes with ($\lambda_s = 0$, $r_s = \pm 1$), such that $\frac{1}{2}\Sigma_s' r_s$ = topological charge, by the index theorem. Eq. (3.23) shows that this latter relation is approximately valid on the lattice, for large β. We will now illustrate that also the spectrum $\{\lambda_s, r_s\}$ on the lattice, approaches the continuum form for $\beta \to \infty$.

In fig. 5 we show the pairs $(a\lambda_s, r_s)$, plotted as coordinates, for the 10 smallest positive eigenvalues. Fig. 5a shows the spectrum of the continuum Dirac operator for a constant field strength gauge field with $Q_v = 1$ [7]. Fig. 5b shows the spectrum

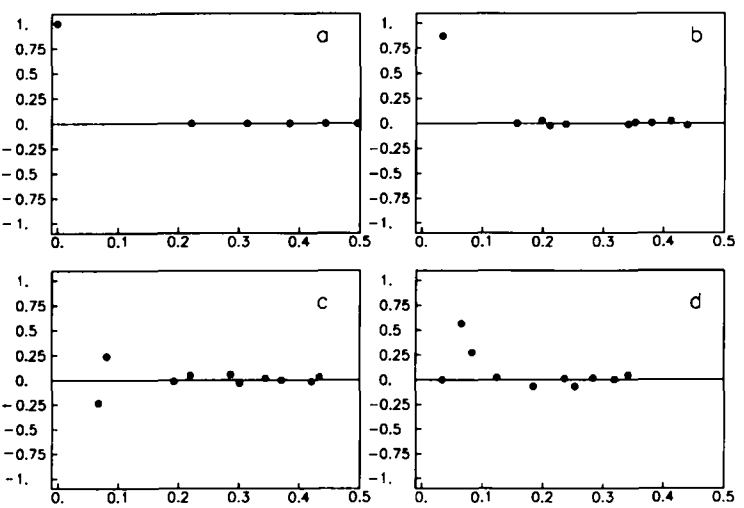

Fig. 5. Spectrum of $\not{\phi}$. The dots represent (λ_s, r_s) for the 10 smallest positive eigenvalues. (a) is for a continuum spectrum, (b, c) for $\beta = 8$, $N = 16$ and (d) for $\beta = 3$, $N = 16$.

obtained from a typical non trivial lattice gauge field at $\beta = 8$ ($N = 16$). The zero mode is quite pronounced. This is a common feature of most configurations; we find $\langle |r_0| \rangle = 0.84$ (± 0.02) and $\langle a\lambda_0 \rangle = 0$ (± 0.039), where the numbers between brackets are the standard deviations. Note that the typical fluctuations of r_0 are much less than the difference $1 - \langle |r_0| \rangle$.

There are configurations, even at this rather large value of β, for which the distinction between zero modes and non-zero modes is less sharp. Fig. 5c shows a relatively rare spectrum with two modes that have $|r_s| \approx 0.25$, somewhere in between zero and $\langle |r_0| \rangle$. This seems to happen in particular when two "zero modes" have opposite residues r_s.

At large β one would hope to see a restoration of flavour symmetry in the physical part of the spectrum, i.e. the small eigenvalues, $|a\lambda| = O(\beta^{-1/2})$, should become doubly degenerate. In particular this would imply that the pairs of zero modes become degenerate and therefore zero. For example, in fig. 5b the zero modes (λ_0, r_0) and $(-\lambda_0, r_0)$ (the latter is not shown in the figure) can be interpreted as two flavour partners that have split up from (0, 1). If the zero mode shift is taken as a measure for the generic eigenvalue shifts, it is clear that the spectrum of fig. 5b does not show flavour symmetry: the typical level splitting is larger than the distance between the levels. Fig. 5c on the other hand, does seem to show an approximate doubly degenerate spectrum. Even the two "reluctant zero modes" can be considered as flavour partners corresponding to continuum degenerate non-zero modes with $r_s = 0$.

Similar ambiguities become more frequent when the gauge field is less smooth. As an example we show in fig. 5d a spectrum obtained from a gauge field at $\beta = 3$ ($N = 16$). Here the distinction between zero modes and non-zero modes becomes somewhat artificial. Fig. 5d also illustrates that the zero modes are not necessarily the modes with the smallest eigenvalues. On large lattices the spectrum becomes increasingly dense and there are bound to be non-zero modes (characterized by a small $|r_s|$) that have an eigenvalue $|\lambda_s|$ smaller than the typical zero mode shift.

Inspired by the effective restoration of the index theorem for large β, one could define an integer charge Q_z on the lattice

$$Q_z = n_+ - n_- \tag{3.25}$$

with n_+ (n_-) the number of zero modes with sign $(r_0) = +$ $(-)$. This evidently leads to $Q_z = n_+ - n_- = Q_t$ for large β. For smaller β one is caught in the problem of recognizing the zero modes, which makes the definition (3.25) ambiguous. In this work we have adopted the criterion (3.17).

3.5. SUSCEPTIBILITY

One can define a scaling window $y'_- < am < y'_+$ around y_0 for the susceptibility

$$\chi_{\text{int}} = \langle Q^2_{\text{int}} \rangle L^{-2}, \tag{3.26}$$

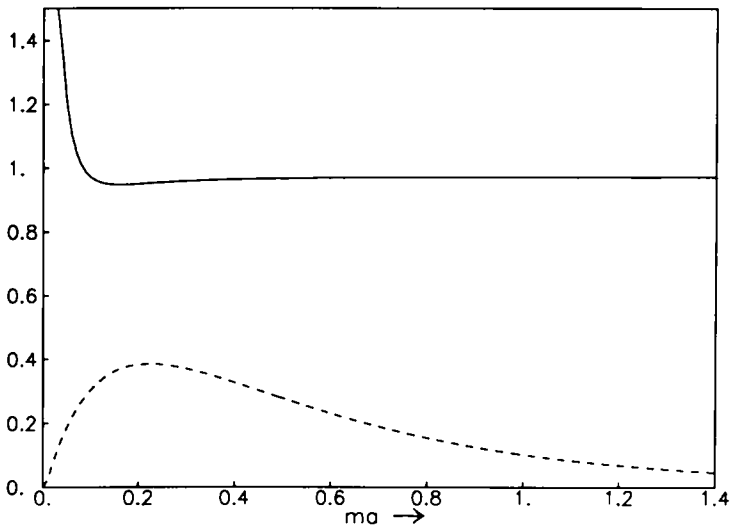

Fig. 6. Mass dependence of χ_{int}. The full curve represents $\chi_{\text{int}} = \langle Q_{\text{int}}^2 \rangle L^{-2}$. The dashed curve represents the unrenormalized susceptibility $\hat{\chi} = \langle \hat{Q}^2 \rangle L^{-2}$. Both susceptibilities are normalized by χ_t.

in which χ_{int} varies less than a fraction δ. The mass dependence of χ_{int} for $\beta = 4$ is shown in fig. 6. The m-independence of most Q_{int}'s for $am \gtrsim y_-$ anticipated that $y'_+ = \infty$. for the lower boundary it appears that y'_- is somewhat smaller than y_-, which confirms the impression that the zero mode shift effect for most Q_{int}'s is reduced by the renormalization (3.18). Since $\chi_{\text{int}} \approx$ const. for $am > y'_-$ we can choose $am = y_-$ and define (cf. (3.22))

$$\bar{\chi} = \langle \bar{Q}^2 \rangle L^{-2}. \tag{3.27}$$

Alternatively one could choose $am = \infty$ and find (for $\beta \gtrsim 2$),

$$\bar{\chi} \approx \chi_{\text{int}}(am = \infty) = \bar{\chi}_n. \tag{3.28}$$

For $am < y'_-$ there is noise due to the zero mode shift fluctuations and χ_{int} increases.

Fig. 7 shows the β-dependence of $\bar{\chi}$. It confirms that $\bar{\chi} \approx \chi_t$ (within statistical errors). Only at small β there is some enhancement of $\bar{\chi}$ due to the increased fluctuations of $\bar{Q}$. For the sake of completeness we have also plotted the susceptibility of Q_z defined in (3.25). For $\beta \gtrsim 2$ this susceptibility is close to χ_t; for $\beta = 1$ it is

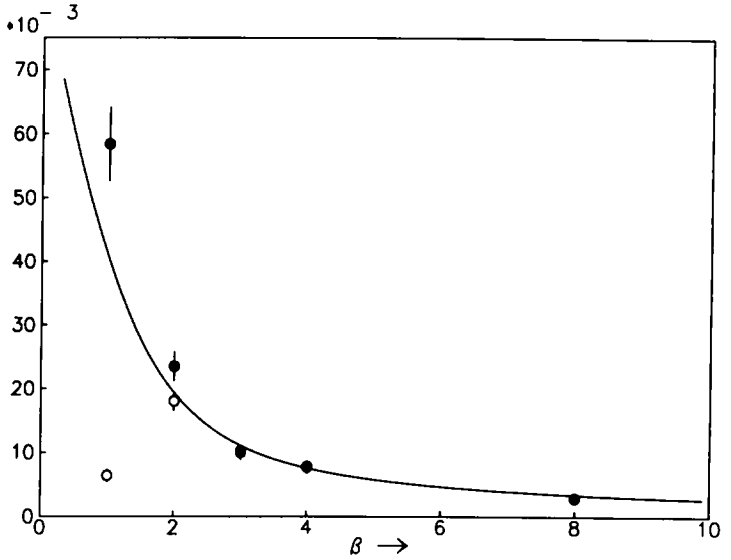

Fig. 7. Susceptibilities. Shown are the renormalized susceptibility $\bar{\chi}$ (indicated by ●) and the "zero mode" susceptibility $\langle (n_+ - n_-)^2 \rangle L^{-2}$ (indicated by ○). The full curve represents χ_t.

too low, indicating that not all zero modes are recognized with the extremely liberal criterion (3.17).

4. Conclusion

For compact QED_2 without fermions we have presented exact results for the "naive" and "topological" susceptibilities χ_n, χ_t and for the string tension σ. These results enabled us to expose a scaling behaviour for these quantities for $\beta \gtrsim 2$ and we could explicitly verify that finite size effects are negligible for $N \gtrsim 3\sqrt{a^2\sigma}$. The exact expressions for $\chi_{t,n}$ could be written in a form elucidating the role of topological sectors (cf. appendix). The "usual" perturbation theory, stemming from the non-compact definition of the model, only incorporates the $Q = 0$ sector, but this still leads to the correct answer for χ_t in the infinite volume limit [4]. This suggests that χ_t can be viewed in two different ways: as a quantity that measures the fluctuations of the charge $\Sigma_x q_t(x)$, which is a property of the gauge field as a whole. Or as the summed correlation function $\langle q_t(x) q_t(0) \rangle$ which has a range of a few correlation lengths. In QED_2 it is ultra local for $N = \infty$: $\langle q_t(x) q_t(0) \rangle = 0$ for $x \neq 0$, and an estimate of $\Sigma_x \langle q_t(x) q_t(0) \rangle$ can be obtained from even a single typical equilibrium gauge field irrespective of the charge of this gauge field. QED_2 and QCD may be similar in this respect [2, 4, 13, 14].

The "fermionic" topological charge $\hat{Q}$ suffers from the zero mode shift effect (for $m \to 0$) and the non-zero mode contributions (for $m \to \infty$). Both effects disappear in

a scaling window $y_-(\beta)a^{-1} < m < y_+(\beta)a^{-1}$ which appears to enlarge to $0 < m < \infty$ for $\beta \to \infty$. In this extremely large-β regime there is no further renormalization of $\hat{Q}$ necessary: $\hat{Q} \approx \text{integer} = Q_t$ provided that the lattice size is such that $\langle Q_t^2 \rangle = O(1)$. For smaller values of β, we could successfully apply the renormalization procedure proposed in [2,3,7]. This finite m-dependent renormalization virtually cancels the m-dependence for m outside the zero mode shift region. The renormalized charge Q_{int} interpolates between the region of zero mode dominance where $Q_{\text{int}} \simeq (n_+ - n_-)$ and the large m region where $Q_{\text{int}} \approx \overline{Q}_n$. The success of the renormalization could be anticipated by generalizing the properties of Q_n to a family of "naive" charges $Q_n^{(k)}$. In QED_2 they presumably are all healthy candidates to measure the susceptibility: for $\beta \to \infty$, $\chi_n^{(k)} \to \chi_t$, $(N = \infty)$. Summarizing, one may state that the "naive", "topological" and "fermionic" definition of topological charge (after a finite renormalization) lead to the same susceptibility, for $\beta \gtrsim 2$.

The spectrum of $\not{D}$ was seen to support the features that lead in the continuum to the index theorem, up to some modifications. At finite β the zero modes have only approximately zero eigenvalues and the zero mode residues are reduced. This reduction is absorbed by the renormalization procedure. This renormalization is meaningful since the renormalized residues typically have deviations from 1 that are much smaller than the reduction before renormalization.

Finally, we discuss some differences with QCD. There are two main differences. The first concerns the behaviour of the zero mode shift region and the residues r_0 of the zero modes. In QED_2 we have found that $1 - \langle |r_0| \rangle \propto a^2$ for $a \to 0$; $y_- a^{-1}$ also appears to vanish for $a \to 0$ but it is not clear at what rate. In any case, for $\beta^{-1} = a^2 g^2$ such that $y_- a^{-1} \ll g$, the renormalization factor for the topological charge, which equals $\langle |r_0| \rangle^{-1}$ in the scaling window, is one. In QCD we expect [3] that the zero mode shift effect is an $O(a^2)$ effect, i.e. $y_- \propto a^2 \Lambda_{\text{QCD}}^2$ for $a \to 0$. However, the zero mode residues will approach 1 much more slowly: $1 - \langle |r_0| \rangle \propto 1/\log a^2$. This implies that the zero mode residues may still differ significantly from one, whereas the zero mode shift region effectively has shrunk to zero. The mass independent renormalization constant κ_P appearing in the definition of topological charge (1.1), cancels this effect: $\kappa_P = \langle |r_0| \rangle^{-1}$, $a \to 0$.

The second difference concerns the naive charge. In QED_2 we have demonstrated that it leads to the correct susceptibility. However, in QCD the analogous charge leads to a divergent susceptibility, $\chi_n \propto a^{-4}$. This implies that also the interpolating charge Q_{int} suffers divergent fluctuations for large m. We have argued [3], that $\langle Q_{\text{int}}^2 \rangle L^{-4}$ evaluated at $am = y_-$, should be finite, with the correct scaling behaviour $\propto \Lambda_{\text{QCD}}^4$.

Appendix

Here we derive expressions for the susceptibilities $\chi_{t,n}$. First the susceptibilities are expressed in terms of the plaquette variables (in this appendix we use $a = 1$ and

omit the subscript 12 on F_{12} and U_{12}),

$$4\pi^2\chi_t = \langle F^2(0)\rangle + \sum_{x\neq 0}\langle F(x)F(0)\rangle$$

$$= \left\langle \sum_{k=0}^{\infty} b_k \mathrm{Re}\,U(0)^k \right\rangle + \sum_{x\neq 0}\left\langle \sum_{kl=1}^{\infty} a_k a_l \mathrm{Im}\,U(x)^k \mathrm{Im}\,U(0)^l \right\rangle, \quad \text{(A.1a)}$$

$$4\pi^2\chi_n = \langle [\mathrm{Im}\,U(0)]^2\rangle + \sum_{x\neq 0}\langle [\mathrm{Im}\,U(0)][\mathrm{Im}\,U(x)]\rangle. \quad \text{(A.1b)}$$

The a_k, b_k are Fourier coefficients,

$$a_k = -2(-1)^k/k, \qquad b_k = 4(-1)^k/k^2, \qquad b_0 = \tfrac{1}{3}\pi^2. \quad \text{(A.2)}$$

Using strong coupling expansion techniques [11] it can be shown that

$$\langle U(x)^k U(0)^l\rangle = \frac{1}{Z}\sum_{n=-\infty}^{\infty} I_{n-k}(\beta) I_{n-l}(\beta) I_n(\beta)^{N^2-2},$$

$$Z = \sum_{n=-\infty}^{\infty} I_n(\beta)^{N^2}. \quad \text{(A.3)}$$

The I_n are the modified Bessel functions of order n. The susceptibility can now be expressed as

$$4\pi^2\chi_t = \frac{1}{Z}\left\{ \tfrac{1}{2}\sum_{n=-\infty}^{\infty}\sum_{k=0}^{\infty} b_k (I_{n-k}+I_{n+k}) I_n^{N^2-1} \right.$$

$$\left. -\tfrac{1}{4}(N^2-1)\sum_{n=-\infty}^{\infty}\left[\sum_{k=1}^{\infty} a_k (I_{n-k}-I_{n+k})\right]^2 I_n^{N^2-2}\right\}, \quad \text{(A.4a)}$$

$$4\pi^2\chi_n = \frac{1}{Z}\left[-\tfrac{1}{4}\sum_{n=-\infty}^{\infty}(I_{n+2}-2I_n+I_{n-2}) I_n^{N^2-1} \right.$$

$$\left. -\tfrac{1}{4}(N^2-1)\sum_{n=-\infty}^{\infty}(I_{n+1}-I_{n-1})^2 I_n^{N^2-2}\right]. \quad \text{(A.4b)}$$

For numerical evaluation, it is convenient to renormalize the Bessel functions as $\tilde{I}_n = I_n/I_0$, since $\tilde{I}_n < 1$ and $\tilde{I}_n^{N^2} \to 0$ rapidly for large N. In the $N\to\infty$ limit the expressions (A.4) simplify, since $\lim_{N\to\infty} N^2\tilde{I}_n^{N^2} = 0$ for $n\neq 0$. Therefore, only the $n=0$ terms contribute, which are zero for the non-local contributions to $\chi_{t,n}$ and after a little rearrangement for χ_n one arrives at formula (2.9) for $N\to\infty$.

The same result (A.4) can be obtained in an alternative way that elucidates the role of the topological sectors and is more accessible in the large β limit. The field strength is used as independent variable and the gauge field average is over all configurations $F(x) \in (-\pi, \pi)$, with the constraint $\Sigma_x F(x) = (\text{integer}) 2\pi$. This constraint follows from the compact nature of F and from the periodic boundary conditions:

$$e^{-i\Sigma_x F(x)} = \prod_x U(x) = \prod_x U_1(x) U_2(x + a_1) U_1^*(x + a_2) U_2^*(x) = e^{-2\pi i Q_t}. \quad \text{(A.5)}$$

The $U_\mu(x)$ are the link variables and the integers Q_t label the topological sectors. Note that these sectors are naturally incorporated in the compact model. For the non-compact model the constraint would inevitably lead to $\Sigma_x F(x) = 0$ and only the zero charge sector would be included. It would take different boundary conditions, e.g. involving transition functions for the gauge field, to include $Q \neq 0$ sectors.

Using $F(x)$ instead of $U_\mu(x)$ is just a change of integration variables. After choosing a complete axial gauge, the $N^2 + 1$ independent $U_\mu(x)$ variables can be replaced by the $N^2 - 1$ $F(x)$ variables; the two remaining $U_\mu(x)$ degrees of freedom represent the value of two orthogonal Polyakov lines. The action does not depend on these degrees of freedom.

All expectation values involving plaquette variables only, can be expressed in terms of the field strengths as follows:

$$\langle G(U) \rangle = \frac{1}{Z} \prod_x \left\{ \int_{-\pi}^{\pi} \frac{dF(x)}{2\pi} \right\} e^{-S'(F)} G(e^{-iF}), \quad \text{(A.6)}$$

where Z is the usual normalization and the constraint is enforced by using the weight

$$e^{-S'(F)} = e^{\Sigma_x \beta(\cos F(x) - 1)} \sum_Q \delta\left(\sum_x F(x) - 2\pi Q \right) \quad \text{(A.7a)}$$

$$= \sum_n e^{\Sigma_x \beta(\cos F(x) - 1) + n \Sigma_x i F(x)}. \quad \text{(A.7b)}$$

Using (A.7b) one immediately recovers (A.3). As stated below (A.4), only the $n = 0$ term contributes for $N \to \infty$. From (A.7b) one then recognizes that the constraint is lost in this limit. It is now easy to compute the correlation functions $\langle F(0) F(x) \rangle$ for $\beta \to \infty$ using a saddle point approximation

$$\langle F(0) F(x) \rangle = \beta^{-1} \delta(x), \quad \text{(A.8)}$$

which verifies that $c_{n,t}(\beta) = 1 + O(\beta^{-1})$ for $\beta \to \infty$. Note that for $N \to \infty$ all

reminiscence of topology has disappeared: $\langle F(0)F(x)\rangle$ is just an (ultra) local correlation function and $\Sigma_x\langle F(0)F(x)\rangle$ can be estimated even from a single typical equilibrium configuration

$$\sum_x \langle F(0)F(x)\rangle = \langle F(0)^2\rangle \approx \frac{1}{N^2}\sum_x F(x)^2, \qquad N \to \infty . \tag{A.9}$$

We would like to thank our colleagues at NIKHEF-H for generous support and computer time on the Gould PN9080. Part of the computations were also performed on the Cyber 205 at SARA with financial support from the "Stichting voor Zuiver Wetenschappelijk Onderzoek (ZWO)". This work is part of the research program of the "Stichting voor Fundamenteel Onderzoek der Materie (FOM)", which is financially supported by ZWO.

References

[1] E. Witten, Nucl. Phys. B156 (1979) 269;
G. Veneziano, Nucl. Phys. B159 (1979) 213
[2] J. Smit and J.C. Vink, Nucl. Phys. B284 (1987) 234
[3] J. Smit and J.C. Vink, Nucl. Phys. B298 (1988) 557
[4] F. Karsch, E. Seiler and I.O. Stamatescu, Nucl. Phys B271 (1986) 349
[5] M. Bochicchio, G.C. Rossi, M. Testa and K. Yoshida, Phys. Lett. 149B (1984) 487
[6] J. Smit and J.C. Vink, Phys. Lett. 194B (1987) 433
[7] J. Smit and J.C. Vink, Nucl. Phys. B286 (1987) 485
[8] J.C. Vink, ITFA-88-2
[9] J. Smit and J.C. Vink, *in*: Lattice gauge theory '86, ed. H. Satz, I. Harrity and J. Potvin (Plenum, 1987)
[10] C. Panagiotakopoulos, Nucl. Phys. B251 [FS13] (1985) 61
[11] J.M. Drouffe and J.B. Zuber, J. Phys. Rep. 102 (1987) 1
[12] S.R. Carson and R.D. Kenway, Ann. Phys. 166 (1986) 364
[13] K. Johnson, *in*: Progress in physics, ed. A. Jaffe, G. Parisi and D. Ruelle, Workshop on Non-perturbative QCD, 1983 (Birkhäuser)
[14] E. Seiler and I.O. Stamatescu, MPI-PAE/PTh 10/87